# A conserved ring of charge in mammalian $Na^+$ channels: a molecular regulator of the outer pore conformation during slow inactivation

Wei Xiong, Yousaf Z. Farukhi, Yanli Tian, Deborah DiSilvestre, Ronald A. Li and Gordon F. Tomaselli

*Molecular and Cellular Cardiology, Department of Medicine, Johns Hopkins University School of Medicine, Baltimore, MD 21205, USA*

**The molecular mechanisms underlying slow inactivation in sodium channels are elusive. Our results suggest that EEDD, a highly conserved ring of charge in the external vestibule of mammalian voltage-gated sodium channels, undermines slow inactivation. By employing site-directed mutagenesis, we found that charge alterations in this asymmetric yet strong local electrostatic field of the EEDD ring significantly altered the kinetics of slow inactivation gating. Using a non-linear Poisson–Boltzmann equation, quantitative computations of the electrostatic field in a sodium channel structural model suggested a significant electrostatic repulsion between residues E403 and E758 at close proximity. Interestingly, when this electrostatic interaction was eliminated by the double mutation E403C + E758C, the kinetics of recovery from slow inactivation of the double-mutant channel was retarded by 2500% compared to control. These data suggest that the EEDD ring, located within the asymmetric electric field, is a molecular motif that critically modulates slow inactivation in sodium channels.**

(Resubmitted 9 June 2006; accepted after revision 24 July 2006; first published online 27 July 2006)
**Corresponding author** G. F. Tomaselli: Department of Medicine, Johns Hopkins University School of Medicine, 720 Rutland Ave/Ross 844, Baltimore, MD 21205, USA. Email: gtomase1@jhmi.edu

The voltage-gated $Na^+$ channel is essential for generation of action potentials in a variety of electrically excitable cells including neurons (Do & Bean, 2003), neuroendocrine, cardiac and skeletal muscle cells. Central to the understanding of ion channel function is elucidating the structural basis of gating and its modulation by a process initiated by S4 movements (Stuhmer *et al.* 1989; Hirschberg *et al.* 1995; Yang & Horn, 1995; Yang *et al.* 1996). $Na^+$ channels conduct ions transiently, and are inactivated rapidly. Inactivation of $Na^+$ channels may occur by one of several kinetically distinct processes referred to as fast, intermediate and slow inactivation, with time constants of recovery of the order of milliseconds, tens to hundreds of milliseconds, and seconds to minutes, respectively (Adelman & Palti, 1969; Ruff *et al.* 1987; Simoncini & Stuhmer, 1987; Kambouris *et al.* 1998).

The clinical significance of slow inactivation in $Na^+$ channels has been validated by abnormalities in slow inactivation that are linked to human neuromuscular diseases such as periodic paralysis (Cummins & Sigworth, 1996; Bendahhou *et al.* 2002) and epilepsy (Alekov *et al.* 2001; Spampanato *et al.* 2004), as well as several potentially lethal cardiac rhythm disorders including Brugada syndrome (Veldkamp *et al.* 2000), long-QT syndrome (Groenewegen *et al.* 2003) and cardiac atrioventricular conduction block (Wang *et al.* 2002). Unlike fast inactivation, however, little is known about the molecular mechanism of slow inactivation in $Na^+$ channels. In *Shaker* $K^+$ channels, C-type inactivation, named because the process is sensitive to mutations in the C-terminal portion of the channel (Hoshi *et al.* 1991), involves a conformational change in the outer vestibule (Yellen *et al.* 1994; Liu *et al.* 1996). Recent studies suggest that slow inactivation may consist of two structurally distinct processes in $K^+$ channels: First, closure of the outer pore, known as P-type inactivation (De Biasi *et al.* 1993; Yang *et al.* 1997); then, stabilization of the closed conformation by C-type inactivation (Olcese *et al.* 1997; Loots & Isacoff, 1998; Pathak *et al.* 2005).

Located C-terminal to the putative DEKA selectivity filter, the outer ring of negatively charged residues Glu-Glu-Asp-Asp (EEDD) is highly conserved in mammalian voltage-gated $Na^+$ channels (Table 1). The local electrostatic potential at the level of the EEDD ring is surprisingly large, more negative than −100 mV (Hui *et al.* 2003). Molecular motions of residues in this ring are coupled to slow inactivation gating based on crosslinking studies of introduced cysteine pairs (Xiong *et al.* 2003). However, the structural mechanism and specific role of EEDD in slow inactivation gating remain

 DOI: 10.1113/jphysiol.2006.115105

**Table 1. The EEDD ring is highly conserved in mammalian $Na^+$ channels**

| rNav | | | hNav | | |
|---|---|---|---|---|---|
| rNav1.1 | | | hNav1.1 | | |
| DI | 378 | LMTQ**D**FW**E**NLYQ | | 378 | LMTQ**D**FW**E**NLYQ |
| DII | 947 | VLCG**E**WI**E**TMWD | | 936 | VLCG**E**WI**E**TMWD |
| DIII | 1428 | VATF**K**GWM**D**IMY | | 1416 | VATF**K**GWM**D**IMY |
| DIV | 1719 | ITTS**A**GW**D**GLLA | | 1709 | ITTSAGW**D**GLLA |
| rNav1.2 | | | hNav1.2 | | |
| DI | 380 | LMTQ**D**FW**E**NLYQ | | 380 | LMTQ**D**FW**E**NLYQ |
| DII | 938 | VLCG**E**WI**E**TMWD | | 938 | VLCG**E**WI**E**TMWD |
| DIII | 1418 | VATF**K**GWM**D**IMY | | 1418 | VATF**K**GWM**D**IMY |
| DIV | 1709 | ITTS**A**GW**D**GLLA | | 1710 | ITTS**A**GW**D**GLLA |
| rNav1.3 | | | hNav1.3 | | |
| DI | 379 | LMTQ**D**YW**E**NLYQ | | 379 | LMTQ**D**YW**E**NLYQ |
| DII | 890 | VLCG**E**WI**E**TMWD | | 939 | VLCG**E**WI**E**TMWD |
| DIII | 1364 | VATF**K**GWM**D**IMY | | 1413 | VATF**K**GWM**D**IMY |
| DIV | 1656 | ITTS**A**GW**D**GLLA | | 1705 | ITTS**A**GW**D**GLLA |
| rNav1.4 | | | hNav1.4 | | |
| DI | 396 | LMTQ**D**YW**E**NLFQ | | 402 | LMTQ**D**YW**E**NLFQ |
| DII | 751 | ILCG**E**WI**E**TMWD | | 757 | ILCG**E**WI**E**TMWD |
| DIII | 1233 | VATF**K**GWM**D**IMY | | 1240 | VATF**K**GWM**D**IMY |
| DIV | 1525 | ITTS**A**GW**D**GLLN | | 1532 | ITTS**A**GW**D**GLLN |
| rNav1.5 | | | hNav1.5 | | |
| DI | 369 | LMTQ**D**CW**E**RLYQ | | 368 | LMTQ**D**CW**E**RLYQ |
| DII | 896 | ILCG**E**WI**E**TMWD | | 894 | ILCG**E**WI**E**TMWD |
| DIII | 1417 | VATF**K**GWM**D**IMY | | 1415 | VATF**K**GWM**D**IMY |
| DIV | 1709 | ITTS**A**GW**D**GLLS | | 1707 | ITTS**A**GW**D**GLLS |
| rNav1.6 | | | hNav1.6 | | |
| DI | 366 | LMTQ**D**YW**E**NLYQ | | 366 | LMTQ**D**YW**E**NLYQ |
| DII | 930 | VLCG**E**WI**E**TMWD | | 932 | VLCG**E**WI**E**TMWD |
| DIII | 1406 | VATF**K**GWM**D**IMY | | 1409 | VATF**K**GWM**D**IMY |
| DIV | 1699 | ITTS**A**GW**D**GLLL | | 1701 | ITTS**A**GW**D**GLLL |
| rNav1.7 | | | hNav1.7 | | |
| DI | 357 | LMTQ**D**YW**E**NLYQ | | 357 | LMTQ**D**YW**E**NLYQ |
| DII | 922 | VLCG**E**WI**E**TMWD | | 933 | VLCG**E**WI**E**TMWD |
| DIII | 1400 | VATF**K**GWM**D**IMY | | 1402 | VATF**K**GWTIIMY |
| DIV | 1692 | ITTS**A**GW**D**GLLA | | 1694 | ITTS**A**GW**D**GLLA |
| rNav1.8 | | | hNav1.8 | | |
| DI | 351 | LMTQ**D**SW**E**RLYQ | | 352 | LMTQ**D**SW**E**RLYQ |
| DII | 844 | ILCG**E**WI**E**NMWV | | 845 | ILCG**E**WI**E**NMWA |
| DIII | 1364 | VATF**K**GWM**D**IMY | | 1363 | VATF**K**GWM**D**IMY |
| DIV | 1658 | ITTS**A**GW**D**GLLS | | 1657 | ITTS**A**GW**D**GLLS |
| rNav1.9 | | | hNav1.9 | | |
| DI | 360 | VMTQ**D**SW**E**RLYR | | 355 | LMTQ**D**SW**E**KLYQ |
| DII | 752 | ILCG**E**WI**E**NMWG | | 764 | ILCG**E**WI**E**NMWE |
| DIII | 1233 | VATY**K**GWL**E**IMN | | 1253 | VATF**K**GWM**D**IIY |
| DIV | 1526 | ITTS**A**GW**D**TLLN | | 1547 | ISTS**A**GW**D**SLLS |

elusive. Here we show that the EEDD ring significantly facilitates the open state of the $Na^+$ channel outer vestibule by, in part, destabilizing outer pore closure that mediates slow inactivation. Neutralization or charge reversal of any residue in this ring markedly favours slow inactivation. Double charge neutralization in the EEDD ring further enhances slow inactivation. The crucial modulation of slow inactivation by this highly conserved outer charged ring suggests that the EEDD ring is a molecular motif regulating the open/closed conformation of the outer vestibule of $Na^+$ channels during slow inactivation.

## Methods

### Molecular mutagenesis and channel expression

A 1.9 kb *Bam*HI–*Sph*I or 2.5 kb *Sph*I–*Kpn*I fragment of the rat $\mu_1$ skeletal muscle $Na^+$ channel (rNav1.4) cDNA (Trimmer *et al.* 1989) was subcloned into pGEM-11Zf$^+$ and pGEM-7Zf$^+$ (Promega, Madison, WI, USA), respectively. Mutagenesis was conducted using the polymerase chain reaction with oligonucleotide primers. Mutations were confirmed by sequencing mutagenic cassettes, which were cloned backed into pSP64T. Complementary RNA was prepared via *in vitro* transcription using SP6 mMessage mMachine kit (Ambion, Austin, TX, USA). Stage V–VI oocytes were harvested from female *Xenopus laevis* that had been anaesthetized by immersion in tank water containing 0.15% tricaine methanesulphonate (pH 7.4; Sigma, St Louis, MO, USA). Adequate anaesthesia was accompanied by the absence of a withdrawal response, typically requiring immersion for 15 min. An additional 5–10 min was required in some animals. Frogs were generally not killed at the end of surgery. They were allowed to recover from anaesthesia and surgery. Agile swimming was required to be observed. After final collection of oocytes, frogs were humanely killed. Animal care and handling followed protocols approved by the Animal Care and Use Committee of the Johns Hopkins University.

The $\alpha$ subunit was coexpressed with the rat brain $\beta_1$ subunit (1 : 1 weight ratio) (Isom *et al.* 1992) in *Xenopus laevis* oocytes as previously described (Tomaselli *et al.* 1995; Benitah *et al.* 1997). Injected oocytes were stored in the following solution (mM): NaCl 96, KCl 2, $MgCl_2$ 1, $CaCl_2$ 1.8, Hepes 5, Pyruvate 5, theophylline 0.5, supplemented with penicillin 100 U ml$^{-1}$ and streptomycin 100 $\mu$g ml$^{-1}$ (pH 7.6 with NaOH) for 1–2 days.

### Molecular model and electrostatic computations

The molecular structure model of the $Na_V1.4$ channel (Lipkind & Fozzard, 2000) and electrostatic isopotential surface were generated with Insight II (MSI, Inc., San Diego, CA, USA). The calculations of electrostatic potentials were performed with DelPhi using a finite difference algorithm and a non-linear Poisson–Boltzmann equation (Gilson & Honig, 1987; Sharp & Honig, 1990). The deepest descents and conjugate gradients were employed for the energy minimization procedures. The dielectric constants were set to 80 for the solvent and 10 for the protein interior. The electrostatic potentials are given in units of $kT/e$, where $k$ is the Boltzmann constant, $T$ is absolute temperature and $e$ is elementary charge. Online data supplementary figures were generated with DeepView.

### Electrophysiology and data analysis

Sodium currents were recorded 24–48 h after injection of cRNA using a two-microelectrode voltage-clamp (OC-725B; Warner Instrument Corp.) from oocytes perfused with frog Ringer solution containing (mM): NaCl 96, KCl 2, $MgCl_2$ 1, Hepes 5 (pH 7.6 with NaOH). All experiments were performed at room temperature. The methanethiosulphonate (MTS) reagents sodium (2-sulphonatoethyl)-methanethiosulphonate (MTSES) and [2-(trimethylammonium)ethyl] methanethiosulphonate bromide (MTSET) were purchased from Toronto Research Chemicals (Ontario, Canada). Acquisition and analysis of whole-cell currents was performed with custom-written software. The voltage-clamp protocols are provided as insets in Figs 2 and 6. The steady-state fast- and slow-inactivation curves were fitted with the Boltzmann function:

$$Y = 1/\{1 + \exp[(V - V_{1/2})/k]\}$$

where $V_{1/2}$ is the midpoint of inactivation and $k$ is the slope factor. The recovery from fast inactivation and development of slow inactivation were fitted with a first-order exponential function of the form:

$$y = y_0 + A[1 - \exp(-t/\tau)]$$

where $A$ is the fractional weight and $\tau$ is the time constant. Recovery from slow inactivation was best fitted with double-exponential function:

$$y = y_o + A_1[1 - \exp(-t/\tau_1)] + A_2[1 - \exp(-t/\tau_2)]$$

Average data are expressed as mean ± S.E.M. Statistical significance was evaluated by ANOVA or unpaired Student's $t$ test (Origin; OriginLab Corp., Northampton, MA, USA) with $P < 0.05$ or $P < 0.01$ representing statistical significance.

## Results

### The EEDD ring

The outer charged ring E403, E758, D1241 and D1532 (Fig. 1) in the external vestibule of rNav1.4 channel is three to four residues C-terminal to the putative selectivity filter DEKA. However, it is highly conserved in mammalian voltage-gated $Na^+$ channels (Table 1). The EEDD ring, serving to concentrate cations in the channel entryway, has recently been shown to be associated with slow-inactivation gating (Xiong *et al.* 2003).

### Neutralization of charged residue destabilizes slow inactivation gating

Figure 2 shows the effects of neutralization of single acidic residues in the outer charged ring on the fast and slow

inactivation in skeletal muscle $Na^+$ channels (rNav1.4). Neutralization of these charged residues individually (E403C, E758C, D1241C or D1532C) produced no significant changes in the steady state channel availability (Fig. 2*A*). Recovery from fast inactivation was not different in these single-cysteine-mutant channels from that in the wild type (Fig. 2*B*). Charge neutralization, however, showed marked enhancement of slow inactivation.

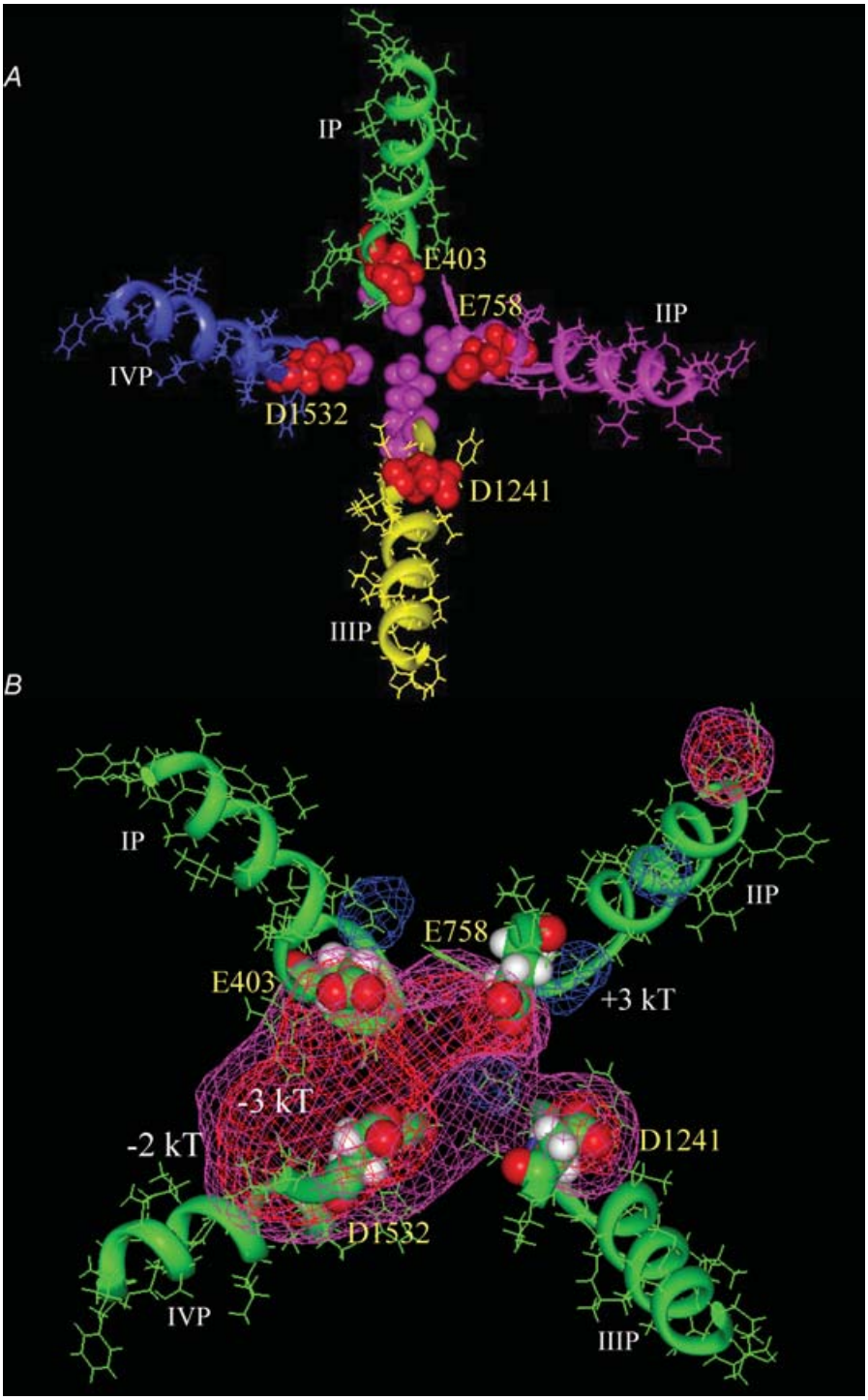


**Figure 1. Molecular structural model of the $Na^+$ channel (Top view)**
*A*, the P-loops of domains I (green), II (pink), III (yellow) and IV (blue) are arranged in a clockwise manner with the outer charged ring (E403, E758, D1241 and D1532) shown in red space-filling format and the selectivity filter shown in pink space-filling format. *B*, the contours of the electrostatic isopotential surfaces at $-2kT$ (purple), $-3kT$ (red) and $+3kT$ (blue) in the $Na^+$ channel outer vestibule are shown. The S5 and S6 segments in domains I–IV were included in electrostatic potential calculations, but were omitted from the figure for clarity.

The development of slow inactivation was significantly facilitated in E403C, E758C, D1241C and D1532C mutant channels (Fig. 2*C*), whereas the recovery from slow inactivation was delayed (Fig. 2*D*). We also observed that slow inactivation, particularly its development, by cysteine substitution at position D1241 was less pronounced when compared with that in other cysteine-mutant channels.

If neutralization of the negative charge in part accounts for the destabilization of the open conformation of the outer pore and enhancement of slow inactivation, then modification of the cysteine substitutions by negatively charged MTS reagents such as MTSES should restore the stabilization of the open state of the channels and retard slow inactivation. Thus, MTSES was applied to these cysteine-mutant channels. Modification by MTSES had no effect on recovery from fast inactivation (Fig. 3*A*). However, MTSES restored the recovery from slow inactivation in E403C, E758C, D1241C and D1532C mutant channels when compared to wild type

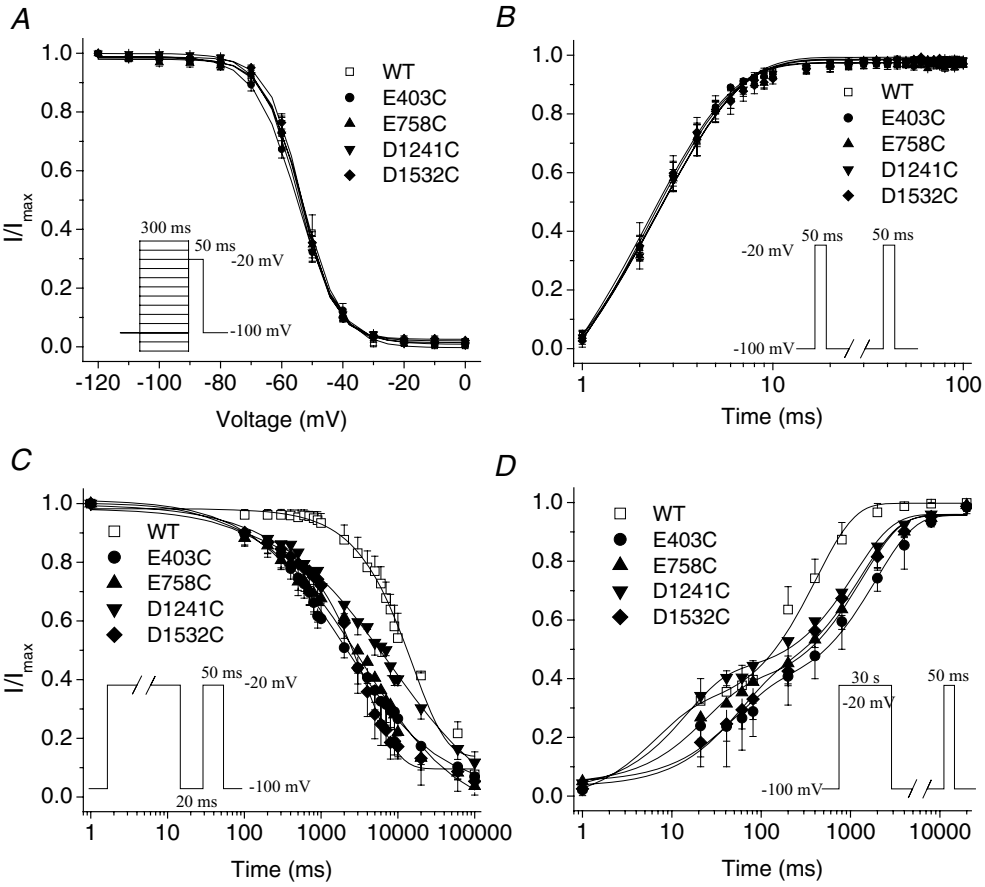


**Figure 2. Characterization of E403C, E758C, D1241C and D1532C mutant channels**
*A*, voltage-dependent fast-inactivation channel availability using the pulse protocol shown in the inset was fitted with Boltzmann distributions for wild type (WT) ($n = 5$), E403C ($n = 14$), E758C ($n = 6$), D1241C ($n = 5$) and D1532C ($n = 8$). The midpoints and slope factors were $-53.03 \pm 1.77$ and $5.95 \pm 0.26$ for WT, $-55.03 \pm 0.98$ and $6.81 \pm 0.45$ for E403C, $-53.89 \pm 1.32$ and $5.42 \pm 0.30$ for E758C, $-54.58 \pm 1.14$ and $5.91 \pm 0.38$ for D1241C, $-53.60 \pm 0.50$ and $5.31 \pm 0.21$ for D1532C. *B*, recovery from fast inactivation was determined using the two-pulse protocol shown in the inset. The data were fitted with a single exponential with time constants as follows: $2.89 \pm 0.30$ WT, $2.47 \pm 0.29$ E403C, $2.70 \pm 0.04$ E758C, $2.60 \pm 0.25$ D1241C and $2.54 \pm 0.35$ D1532C; $n = 4$. *C*, development of slow inactivation using the two-pulse protocol shown in the inset. The interval between each episode is 60 s with a holding potential of $-100$ mV. The time constants ($\tau$) and fractional amplitudes (in parentheses) were as follows: WT, $\tau = 15612 \pm 910$ ms ($0.85 \pm 0.02$); E403C, $\tau = 6846 \pm 2286$ ms** ($0.79 \pm 0.06$); E758C, $\tau = 6587 \pm 1632$ ms** ($0.76 \pm 0.07$); D1241C, $\tau = 9623 \pm 878$ ms** ($0.72 \pm 0.07$); D1532C, $\tau = 3970 \pm 971$ ms** ($0.84 \pm 0.02$); $n = 4$–5. *D*, time course of recovery from slow inactivation using the two-pulse protocol shown in the inset. The interval between each episode is 30 s with a holding potential of $-100$ mV. Time constants and fractional amplitudes (in parentheses) were as follows: WT ($n = 5$), $\tau_1 = 48.28 \pm 37.10$ ms ($0.34 \pm 0.09$), $\tau_2 = 406.87 \pm 87.52$ ms ($0.67 \pm 0.11$); E403C ($n = 5$), $\tau_1 = 45.46 \pm 36.87$ ms ($0.32 \pm 0.04$), $\tau_2 = 2204.03 \pm 698.01$ ms* ($0.64 \pm 0.03$); E758C ($n = 4$), $\tau_1 = 34.29 \pm 19.44$ ms ($0.32 \pm 0.06$), $\tau_2 = 1345.04 \pm 407.00$ ms* ($0.58 \pm 0.05$); D1241C ($n = 5$), $\tau_1 = 11.25 \pm 3.41$ ms ($0.41 \pm 0.04$), $\tau_2 = 1741.49^* \pm 497.12$ ms ($0.63 \pm 0.03$); D1532C ($n = 6$), $\tau_1 = 114.52 \pm 43.41$ ms ($0.42 \pm 0.04$), $\tau_2 = 1707.04^* \pm 387.64$ ms ($0.52 \pm 0.05$). $^*P < 0.05$; $^{**}P < 0.01$.

(Fig. 3*B*). Interestingly, entry into slow inactivation in the presence of MTSES was only partially yet significantly restored in E403C (Fig. 3*C*), but not the other single-cysteine-mutant channels (E758C, D1241C or D1532C, Fig. 3*D–F*). To further test the effect of charge on slow inactivation, the mutant E403C was modified by the positively charged MTSET. MTSET application had no effect on recovery from fast inactivation in E403C mutant channels (Fig. 4*A*). In contrast, despite little alteration in the rate of entry into slow inactivation, recovery from slow inactivation was further delayed in E403C mutant channels (Fig. 4*B–C*). Thus, these results were consistent with the notion that the charge in the ring is an important modulator of slow inactivation, particularly the recovery from slow inactivation.

### Charge reversal further destabilizes slow inactivation

If neutralization of one negative charge in the EEDD ring reduced the electrostatic repulsion, it is possible that charge reversal of a single residue could induce additional constriction of the outer charged ring via electrostatic attraction. Additionally, a different amino acid mutant might reveal changes in gating that result from steric effects. Thus, we substituted each of the negative charges in the EEDD ring with an arginine. No significant changes in steady-state fast inactivation and recovery from fast inactivation were found in E403R, E758R, D1241R and D1532R mutant channels (Fig. 5*A* and *B*). Entry into slow inactivation was hastened in these arginine-mutant channels compared to the wild type

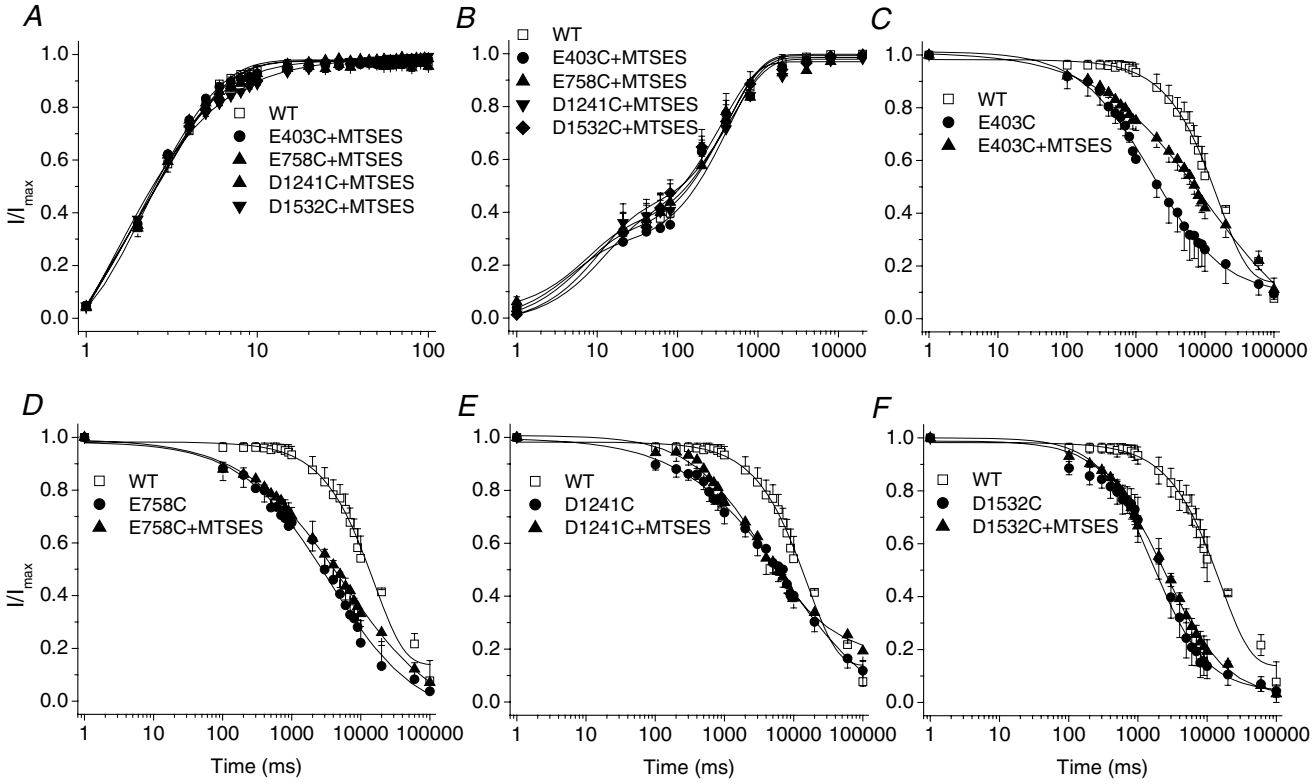


**Figure 3. Effects of the negatively charged MTSES on inactivation gating of single-cysteine-mutant channels**

The voltage-clamp protocols are provided as insets in Fig. 2. *A*, application of MTSES (10 mM) to E403C, E758C, D1241C and D1532C had no effect on recovery from fast inactivation. *B*, MTSES restores the recovery from slow inactivation in these cysteine-mutant channels. Time constants and fractional weights (in parentheses) were as follows: WT ($n = 5$), $\tau_1 = 48.28 \pm 37.10$ ms ($0.34 \pm 0.09$), $\tau_2 = 406.87 \pm 87.52$ ms ($0.67 \pm 0.11$); E403C + MTSES: ($n = 6$), $\tau_1 = 19.82 \pm 15.46$ ms ($0.33 \pm 0.06$), $\tau_2 = 608.06 \pm 213.27$ ms ($0.62 \pm 0.09$); E758C + MTSES ($n = 5$), $\tau_1 = 5.67 \pm 2.34$ ms ($0.36 \pm 0.07$), $\tau_2 = 561.18 \pm 162.06$ ms ($0.66 \pm 0.08$); D1241C + MTSES ($n = 3$), $\tau_1 = 4.13 \pm 1.39$ ms ($0.42 \pm 0.11$), $\tau_2 = 401.63 \pm 53.97$ ms ($0.63 \pm 0.05$); D1532C + MTSES ($n = 4$), $\tau_1 = 31.79 \pm 7.41$ ms ($0.40 \pm 0.06$), $\tau_2 = 416.86 \pm 40.58$ ms ($0.63 \pm 0.05$). *C–F*, MTSES did not slow the kinetics of the development of slow inactivation with the exception of the partial restoration in E403C (*C*). The time constants were $12738 \pm 1154$ ms* (*C*, E403C + MTSES, $n = 4$), compared with $6846 \pm 2286$ ms (E403C); $7914 \pm 567$ ms (*D*, E758C + MTSES, $n = 4$), compared with $6587 \pm 1632$ ms (E758C); $8969 \pm 1223$ ms (*E*, D1241C + MTSES, $n = 3$), compared with $9623 \pm 878$ ms (D1241C); and $4058 \pm 869$ ms (*F*, D1532C + MTSES, $n = 4$), compared with $3970 \pm 970$ ms (D1532C). *$P < 0.05$.

(Fig. 5*C*); however, enhancement of the development of slow inactivation was no greater than that produced by charge neutralization with single-cysteine-mutant substitutions (E403C *versus* E403R, E758C *versus* E758R, D1241C *versus* D1241R and D1532C *versus* D1532R) (Figs 5*C* and 3*C*) (n.s.). In contrast, recovery from slow inactivation was generally further delayed in arginine substitution mutants, compared with the single-cysteine-mutant channels (Fig. 5*D–F*). The time constants of recovery from slow inactivation of E758R ($2627 \pm 152$ ms) and D1532R ($5077 \pm 942$ ms) were significantly longer than those for E758C ($1345 \pm 407$ ms) and D1532C ($1707 \pm 388$ ms), respectively ($P < 0.05$). The time constants of recovery from slow inactivation of E403R ($3276 \pm 1173$) and D1241R ($2640 \pm 521$ ms) tended be longer than those for E403C ($2204 \pm 698$ ms) and D1241C ($1741 \pm 497$ ms), but the difference did not reach statistical significance.

### Slow inactivation in $Na^+$ channels: two successive steps?

Mutations changing the charge of the EEDD ring significantly altered entry into slow inactivation. However, we found that in comparison with recovery from slow inactivation, rates of entry into slow inactivation were relatively less sensitive to charge alterations. Both charge neutralization and reversal similarly slowed entry into slow inactivated states. Modification of single-cysteine mutants by negatively charged MTSES nearly completely restored recovery from slow inactivation, but had little effect on the development of slow inactivation in the majority of these cysteine-mutant channels, with the exception of partial restoration in E403C (Fig. 3*B–F*). In addition, charge reversal had potent effects on the kinetics of recovery, but not the kinetics of the development of slow inactivation when compared with charge neutralization mutants (Figs 2*C* and 5*C*). Taken together, these results suggest that entry into slow inactivation, and recovery from slow inactivation involve different structural rearrangements and are not simply forward and reverse processes. Recovery from slow inactivation may contain an additional component that is very sensitive to charge.

### Double charge neutralization and enhanced slow inactivation

If neutralization of a single amino acid in the EEDD ring could destabilize the open conformation of the slow inactivation gate, double cysteine mutations might produce further destabilization. The voltage dependence and kinetics of recovery from fast inactivation were not altered in E403C + E758C, E403C + D1241C, E403C + D1532C, E758C + D1532C and D1241C + D1532C mutant channels compared with wild-type or single-cysteine-mutant channels (Fig. 6). The steady-state slow inactivation curve shows that in wild-type channels approximately 20% of channels did not slow inactivate (Fig. 7), a finding consistent with other reports (Featherstone *et al.* 1996; Richmond *et al.* 1998). With the exception of D1532R ($V_{1/2} = -62.0 \pm 3.1$ mV

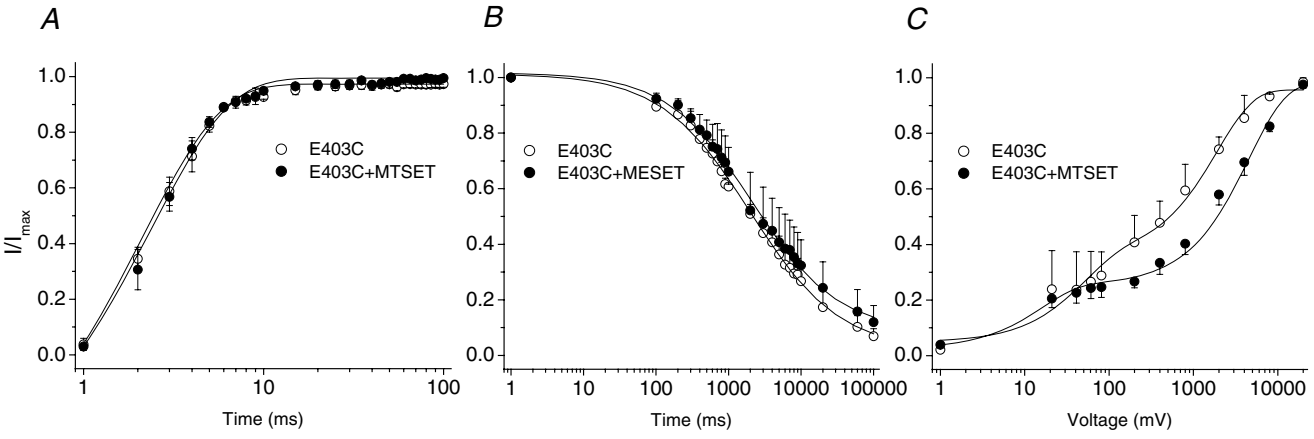


**Figure 4. Modification of E403C channel kinetics by positively charged MTSET**
The voltage-clamp protocols are provided as insets in Fig. 2. *A*, the kinetics of recovery from fast inactivation remained unchanged by application of MTSET (1 mM). *B*, the time constant of entry into slow inactivation was not altered ($6254.66 \pm 1844.07$ ms in the presence of MTSET, compared with $6846.42 \pm 2285.78$ ms for control). $n = 3$–4. *C*, the kinetics of recovery from slow inactivation were impeded by MTSET. Time constants and fractional amplitudes (in parentheses) were as follows: E403C + MTSET ($n = 9$), $\tau_1 = 15.8 \pm 7.0$ ms ($0.23 \pm 0.02$), $\tau_2 = 4598 \pm 465$ ms* ($0.73 \pm 0.02$); compared with E403C ($n = 5$), $\tau_1 = 45.5 \pm 37$ ms ($0.32 \pm 0.04$), $\tau_2 = 2204 \pm 698$ ms ($0.64 \pm 0.03$). *$P < 0.05$.

*versus* $-53.7 \pm 1.58$ mV in wild type, $P < 0.01$), the single-mutant channels did not produce significant changes in the steady-state slow inactivation curves (Fig. 7*A* and *B*, Table 2). In contrast, most of the double-cysteine-mutant channels exhibited significant changes in $V_{1/2}$, slope factor and residual currents (Fig. 7*C*, Table 2). The E403C + E758C, E758C + D1532C and D1241C + D1532C channels exhibited an approximately 10–20 mV shift of the $V_{1/2}$ in the hyperpolarized direction, a reduction in slope factor and more complete slow inactivation (92–100% *versus* 80% for the wild type).

The kinetics of entry into slow inactivation were significantly enhanced compared with the wild type (Fig. 8*A*). However, there was no difference in time constants of the development of slow inactivation between these double-mutant channels and

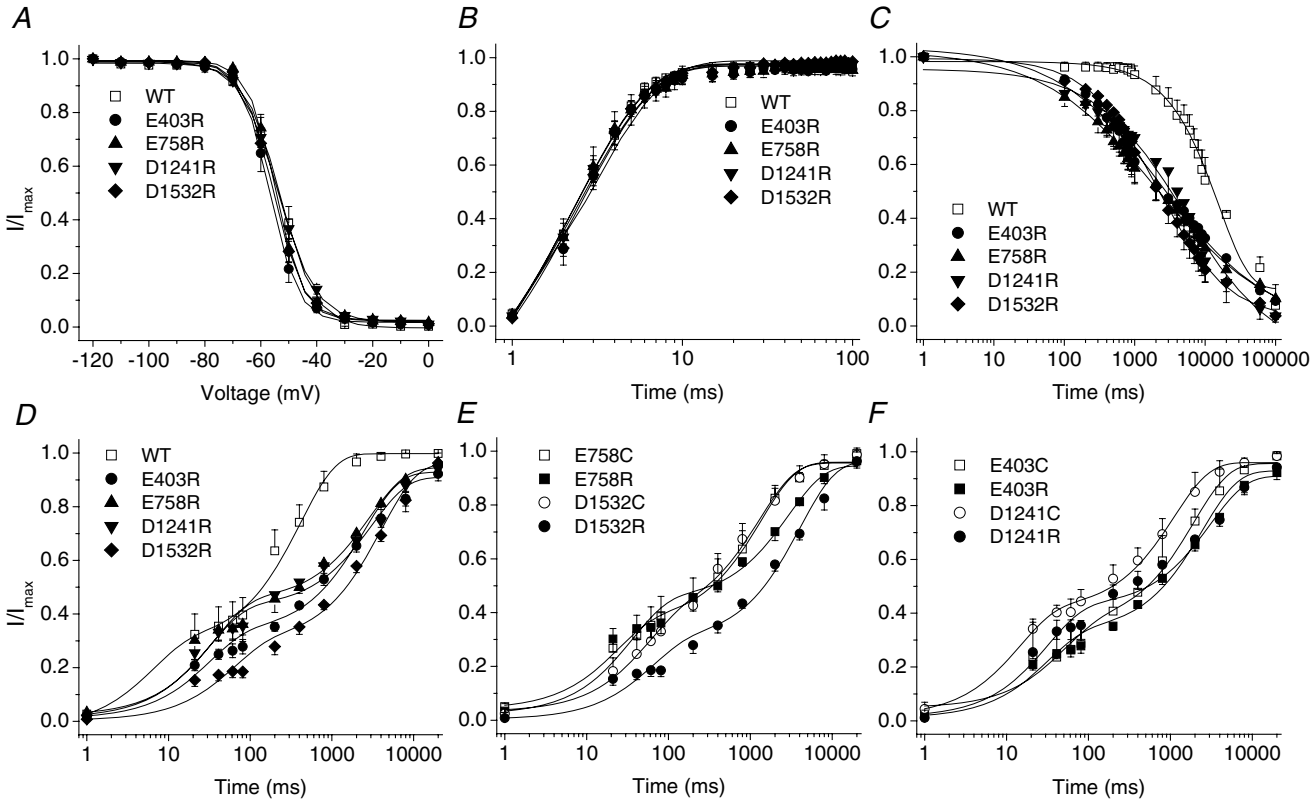


**Figure 5. Charge reversal facilitates slow inactivation**
The voltage-clamp protocols are provided as insets in Figure 2. *A*, steady state fast-inactivation channel availability was not changed by substitution of external ring residues with arginine. The data were fitted as described in Fig. 2. The midpoints and slope factors were $-55.5 \pm 1.5$ and $4.5 \pm 0.3$ E403R ($n = 6$), $-55 \pm 1.3$ and $4.5 \pm 0.3$ E758R ($n = 5$), $-54.2 \pm 1.2$ and $5.2 \pm 0.2$ D1241R ($n = 15$) and $-55.5 \pm 1.0$ and $5.3 \pm 0.1$ D1532R ($n = 7$); compared with $-53.0 \pm 1.2$ and $6.0 \pm 0.3$ WT, respectively. *B*, recovery from fast inactivation was unaltered by charge reversal. The time constants were $2.6 \pm 0.2$ (E403R), $2.5 \pm 0.5$ (E758R), $2.5 \pm 0.1$ (D1241R) and $2.5 \pm 0.3$ (D1532R), $n = 4$–5; compared with $3.0 \pm 0.3$ (WT). *C*, development of slow inactivation was significantly enhanced. The data were fitted in each case by a single exponential, $n = 4$–6. The time constants and fractional weights (in parentheses) were $3852 \pm 1564$ ms** ($0.7 \pm 0.02$) for E403R, $4564 \pm 1294$ ms** ($0.7 \pm 0.0$) for E758R, $7998.54 \pm 1959.13$ ms** ($0.81 \pm 0.02$) for D1241R, $6898 \pm 1009$ ms** ($0.8 \pm 0.03$) for D1532R; compared with $15612 \pm 910.$ ms and $0.1 \pm 0.02$ (WT). *D*, charge reversal further impaired the kinetics of recovery from slow inactivation. The data were best fitted with two-order time constants. The time constants and fractional weight were: $\tau_1 = 59.2 \pm 24.8$ ms ($0.3 \pm 0.03$), $\tau_2 = 3276 \pm 1173$ ms** ($0.5 \pm 0.02$) for E403R ($n = 5$); $\tau_1 = 33.8 \pm 13.5$ ms ($0.4 \pm 0.04$), $\tau_2 = 2627 \pm 152$ ms** ($0.5 \pm 0.04$) for E758R ($n = 4$); $\tau_1 = 17.4 \pm 6.7$ ms ($0.4 \pm 0.05$), $\tau_2 = 2640 \pm 521$ ms** ($0.5 \pm 0.04$) for D1241R ($n = 3$); $\tau_1 = 169 \pm 94.4$ ms ($0.3 \pm 0.03$), $\tau_2 = 5077 \pm 942$ ms** ($0.7 \pm 0.04$) for D1532R ($n = 6$); compared with $\tau_1 = 48.3 \pm 37.1$ ms ($0.34 \pm 0.10$), $\tau_2 = 407 \pm 87.5$ ms ($0.7 \pm 0.1$) for WT ($n = 5$). *E*, E758R and E1532R mutant channels exhibited extra delay in recovery from slow inactivation compared with E758C and E1532C, respectively ($P < 0.05$). *F*, comparison of the effects of E403R and E1241R mutations on the recovery from slow inactivation with those of E403C and E1241C substitution, respectively (n.s.). *$P < 0.05$, **$P < 0.01$.

single-cysteine- or -arginine-mutant channels, suggesting that the development of slow inactivation is less sensitive to alterations in charge. In contrast, the recovery from slow inactivation was markedly impaired with the most dramatic delay observed in E403C + E758C mutant channels (Fig. 8*B*). Figure 8*C* summarizes the time constants of recovery from slow inactivation (the slower time constant of the two-component recovery) of double mutant channels that were increased 5–10 fold compared with wild-type channels. There was a 25-fold increase in the E403C + E758C mutant.

In addition, we examined the effects of extracellular $Na^+$ concentration on gating of E403C + E758C mutant channels. Steady-state fast inactivation was not altered by increasing the $Na^+$ concentration (online Supplementary Fig. 1*A*). However, the steady-state slow inactivation curve was shifted in the hyperpolarizing direction with higher extracellular $Na^+$ concentration (online Supplementary Fig. 1*B*). Despite minimal changes in entry into slow inactivation, recovery from slow inactivation was facilitated, consistent with inhibition of slow inactivation in the presence of higher extracellular $Na^+$ concentration (online Supplementary Fig. 1*C–D*) (Townsend & Horn, 1997).

## Discussion

### Slow inactivation in $Na^+$ channels

Voltage-dependent ion channels exhibit multiple kinetically and mechanistically distinct forms of inactivation. In *Shaker* $K^+$ channels, N-type inactivation is mediated by an intracellular region at the amino-terminus acting as a tethered 'ball' occluding the pore (Hoshi *et al.* 1990). *Shaker* $K^+$ channels also exhibit C-type inactivation that is affected by mutations in the S6 segments (Hoshi *et al.* 1991; Boland *et al.* 1994). C-type inactivation is impaired by application of TEA to the extracellular side of the channels, whereas intracellular application affects N-type inactivation (Choi *et al.* 1991). In *Shaker* $K^+$ channels, a consensus has been reached that C-type inactivation is associated with constriction of the outer pore related to structural rearrangements in the P-segments (Yellen *et al.* 1994; Liu *et al.* 1996; Harris *et al.* 1998; Kiss & Korn, 1998), although the precise molecular nature of this inactivation gate is not clear. However, similar to our data, a recent study revealed the interesting observation that P-loop mutants drastically affect C-type inactivation gating in KcsA channels (Cordero-Morales *et al.* 2006). In KcsA channels,

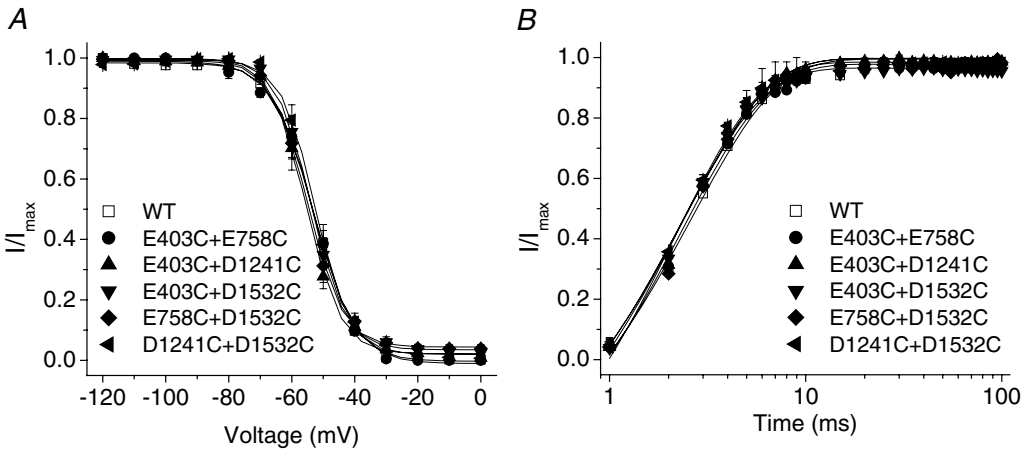


**Figure 6. Double cysteine substitution has little effect on the kinetics of fast inactivation**
The voltage-clamp protocols are provided as insets in Figure 2. *A*, voltage dependence of steady-state fast inactivation of the double mutants did not differ from the wild type. The data were fitted with a Boltzmann equation with midpoints (mmV) of $-54.2 \pm 1.2$, $-55.2 \pm 1.0$, $-53.7 \pm 1.4$, $-55.3 \pm 1.8$ and $-52.7 \pm 1.4$, and slope factors (mV) of $6.7 \pm 0.6$, $5.5 \pm 0.2$, $5.5 \pm 0.2$, $5.2 \pm 0.4$, $5.2 \pm 0.2$ for E403C + E758C ($n = 4$), E403C + D1241C ($n = 8$), E403C + D1532C ($n = 9$), E758C + D1241C ($n = 5$), D1241C + D1532C ($n = 4$), respectively; compared with $53.0 \pm 1.8$ and $6.0 \pm 0.3$ for WT ($n = 5$). *B*, kinetics of recovery from fast inactivation in double-mutant channels were not changed compared with the wild type. The time constants were $2.5 \pm 0.1$ ms, $2.43 \pm 0.2$ ms, $2.3 \pm 0.1$ ms, $2.5 \pm 0.4$ ms and $2.2 \pm 0.1$ ms for E403C + E758C ($n = 5$), E403C + D1241C ($n = 7$), E403C + D1532C ($n = 5$), E758C + D1241C ($n = 3$), D1241C + D1532C ($n = 4$), respectively; compared with $2.4 \pm 0.04$ for WT.

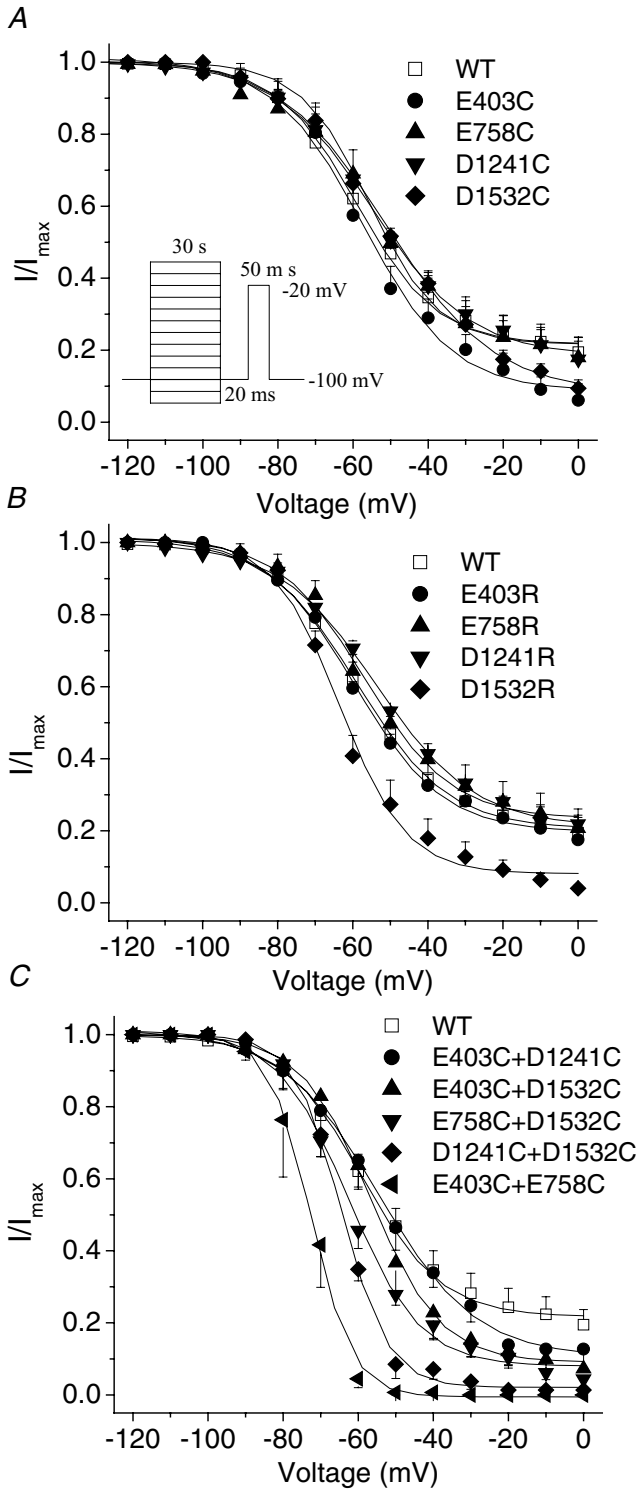


**Figure 7. Voltage dependence of steady-state slow inactivation of single-mutant and double-cysteine-mutant channels**
Voltage-dependent slow-inactivation channel availability using the pulse protocol shown in the inset was fitted with a Boltzmann equation. The interval between each episode is 30 s with a holding potential of −100 mV. *A–C*, the midpoints, slope factors and components of non-inactivated channels of Boltzmann curves are listed in Table 2. D1532R was the only single mutant showing significant changes in voltage-dependent slow-inactivation channel availability (*B*), whereas E403C + D1421C was the only double mutant that did not show any significant changes in voltage dependence of steady-state slow inactivation compared with wild-type channels. E403C + E758C showed the most profound changes in midpoints, slope factors and components of non-slow-inactivated channels of Boltzmann curves (*C*).

Glu71 forms a strong interaction with Asp80 located at the end of Gly-Tyr-Gly-Asp signature sequence (Zhou *et al.* 2001). The E71A mutation significantly alters the C-type inactivation by eliminating its interaction with Asp80 and thus initiating further conformational changes in the P-loop that stabilize the open state (Cordero-Morales *et al.* 2006).

In $Na^+$ channels, fast inactivation is mediated by the cytoplasmic III–IV linker that functions as a tethered pore blocker binding to an inactivation gate receptor in the intracellular mouth of the channel (Vassilev *et al.* 1989; Patton *et al.* 1992; West *et al.* 1992). The structural basis of slow inactivation in $Na^+$ channels is much less clear. Mutations located in the regions other than P-loops, including S6 segments, have been described to influence slow inactivation in $Na^+$ channels (Hayward *et al.* 1997; Wang & Wang, 1997; Bendahhou *et al.* 1999; O'Reilly *et al.* 2001; Wang *et al.* 2005). On the other hand, a growing body of evidence suggests that the outer pore of $Na^+$ channels is linked to slow inactivation (Tomaselli *et al.* 1995; Balser *et al.* 1996; Townsend & Horn, 1997; Kambouris *et al.* 1998; Todt *et al.* 1999; Ong *et al.* 2000; Hilber *et al.* 2001; Vilin *et al.* 2001; Hilber *et al.* 2002; Xiong *et al.* 2003; Zhang *et al.* 2003; Fukuda *et al.* 2005; Pavlov *et al.* 2005; Tsang *et al.* 2005). A previous report did not detect a difference in the aqueous accessibility of residues in the outer vestibule between open and inactivated states (Struyk & Cannon, 2002), however, our recent data suggest the accessibility to cysteine-modifying reagents of G1530C and Y401C, located deep in the outer vestibule, is significantly impaired during slow inactivation compared with other channel states (Xiong & Tomaselli, 2005). Taken together, it is most likely that slow inactivation in $Na^+$ channels resembles C-type inactivation in *Shaker* $K^+$ channels (Kass, 2004).

## Does slow inactivation in $Na^+$ channels take place in two steps?

Recent evidence has shown that slow inactivation has two distinct components in *Shaker* $K^+$ channels. The closure of the outer pore, known as P-type inactivation (De Biasi *et al.* 1993; Yang *et al.* 1997), precedes the second step, referred to as 'C-type inactivation', which stabilizes the closed conformation via shifting the voltage dependence of recovery from slow inactivation (Olcese *et al.* 1997; Loots & Isacoff, 1998; Pathak *et al.* 2005). Upon prolonged depolarization, the gate closes and enters into a less stable

**Table 2. Parameters of steady-state slow inactivation of single- and double-mutants**

| | Midpoint (mV) | Slope factor | Component of non-slow inactivated |
|---|---|---|---|
| WT | $-53.6 \pm 1.6$ | $12.0 \pm 1.1$ | $0.20 \pm 0.05$ |
| E403C | $-57.3 \pm 3.5$ | $12.0 \pm 1.8$ | $0.08 \pm 0.04$ |
| E758C | $-56.3 \pm 3.6$ | $12.8 \pm 2.7$ | $0.18 \pm 0.05$ |
| D1241C | $-55.2 \pm 1.5$ | $13.0 \pm 1.0$ | $0.19 \pm 0.05$ |
| D1532C | $-51.3 \pm 0.9$ | $14.4 \pm 1.0$ | $0.08 \pm 0.02$ |
| E403R | $-59.6 \pm 1.8$ | $11.5 \pm 1.3$ | $0.20 \pm 0.03$ |
| E758R | $-57.0 \pm 1.6$ | $11.6 \pm 1.6$ | $0.23 \pm 0.05$ |
| D1241R | $-53.6 \pm 0.6$ | $13.2 \pm 1.7$ | $0.21 \pm 0.04$ |
| D1532R | $-62.0 \pm 3.1^{**}$ | $9.3 \pm 2.2$ | $0.08 \pm 0.01^{*}$ |
| E403C + E758C | $-73.8 \pm 3.3^{**}$ | $4.5 \pm 0.9^{**}$ | $0.00 \pm 0.00^{**}$ |
| E403C + D1241C | $-51.9 \pm 4.4$ | $11.8 \pm 1.1$ | $0.11 \pm 0.07$ |
| E403C + D1532C | $-54.4 \pm 3.1$ | $9.4 \pm 1.7$ | $0.08 \pm 0.02^{*}$ |
| E758C + D1532C | $-62.5 \pm 1.4^{**}$ | $9.4 \pm 0.7^{*}$ | $0.08 \pm 0.02^{*}$ |
| D1241C + D1532C | $-66.1 \pm 2.4^{**}$ | $6.5 \pm 1.1^{**}$ | $0.05 \pm 0.02^{*}$ |

$^{*}P < 0.05$, $^{**}P < 0.01$, $n = 3$–5 oocytes.

P-type inactivation first. Further sustained depolarization leads to a slower entry into more stable C-type inactivation associated with additional rearrangement of or around S4, and a shift in the voltage dependence of the gating charge in the hyperpolarized direction. Therefore, the onset of slow inactivation is time dependent, whereas recovery from slow inactivation becomes intrinsically voltage dependent and involves additional S4 movements (Loots & Isacoff, 1998).

Our data demonstrate that a number of modifications of the outer charged ring in the external channel vestibule (charge neutralization or reversal, charge restoration by MTSES modification) produce significant changes in recovery from slow inactivation. In contrast, charge neutralization altered entry into slow inactivation, but charge restoration or reversal was not associated with additional alterations in the kinetics of the development of slow inactivation. These results suggest that the charged outer ring has a stronger impact on the recovery from slow inactivation ('C-type inactivation') than entry into slow inactivation ('P-type inactivation'), analogous to a two-step slow inactivation in *Shaker* $K^+$ channels. However, it is unclear how the charges in S4 interact with the charges in the EEDD ring in $Na^+$ channels, although in *Shaker* $K^+$ channels, the outermost charge in the S4 (R362) has been shown to interact with the outer pore domain, generating an allosteric effect on slow inactivation (Loots & Isacoff, 2000; Elinder *et al.* 2001).

## The role of electrical charge in modulation of slow inactivation

The outer negatively charged ring EEDD located at three to four amino acid residues external to the selectivity filter DEKA is highly conserved in the mammalian voltage-gated $Na^+$ channels (Table 1). The local electrostatic potential at the level of the outer charged ring EEDD has been estimated to be $-92.8$ to $-117$ mV (Khan *et al.* 2002; Hui *et al.* 2003), with a lower-limit estimate of $-58$ to $-65$ mV (Green *et al.* 1987; Khan *et al.* 2002). Neutralization of one of these residues enhanced slow inactivation.

A previous report found that only E758C significantly disrupted the kinetics of slow inactivation, but three other cysteine substitutions in this ring, namely E403C, D1241C and D1532C, did not (Struyk & Cannon, 2002). However, the relatively brief depolarization period of 3 s at $-10$ mV used in this study (Struyk & Cannon, 2002) may have been insufficient to induce slow inactivation (Vilin *et al.* 1999; Ong *et al.* 2000; Tsang *et al.* 2005). In contrast, E403C has been shown to hasten recovery from slow inactivation and enhance entry into slow inactivation (Zhang *et al.* 2003), consistent with our findings. In our study, restitution of negative charge with MTSES reagents in E403C, E758C, D1241C and D1532C mutant channels restored the recovery from slow inactivation to that of wild-type channels. Reversal of the negative charge of the side chain further facilitated slow inactivation. Some of the double-cysteine mutants such as E403C + E758C drastically enhanced slow inactivation. The time constant of recovery from slow inactivation was increased by 2500%. The strong electrical repulsion present between E403 and E758 at close proximity in the wild-type channel vanishes in the double-mutant channel (Fig. 9). Thus, it is likely that these double mutations would permit a change in the spatial relationship between these two residues and others within the outer pore, facilitating constriction of the external vestibule and channel closure.

The effects of charge neutralization and reversal in the EEDD ring and altered extracellular $Na^+$ concentration on slow inactivation are consistent with a significant electrostatic contribution to this gating process. However, shielding of electrostatic potential is only one of several

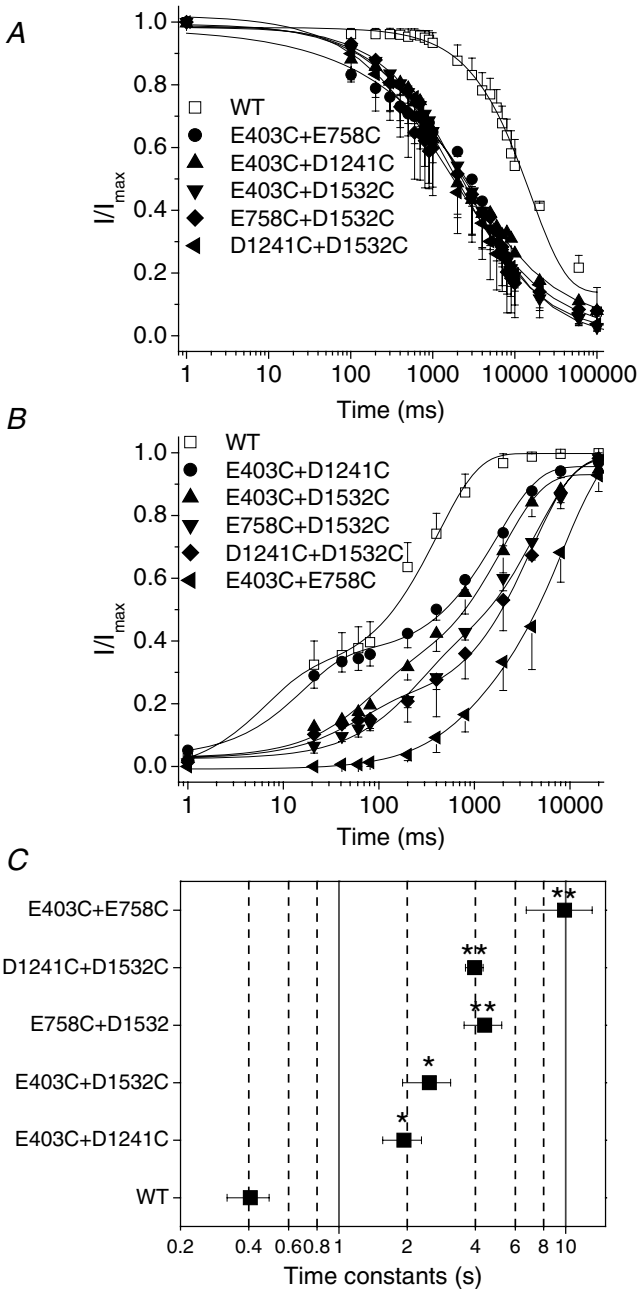


**Figure 8. Double cysteine mutations in the EEDD ring exhibit marked enhancement of slow inactivation**

The voltage-clamp protocols are provided as insets in Figure 2. *A*, the double mutants hastened the kinetics of the development of slow inactivation. The data were fitted with a single exponential. The time constants and fractional weight were 4054.97 ± 654.00 ms** and 0.7 ± 0.06 for E403C + E758C, 512 ± 1537 ms** and 0.8 ± 0.06 for E403C + D1241C, 5017 ± 819 ms** and 0.9 ± 0.02 for E403C + D1532C, 3867 ± 2085 ms** and 0.8 ± 0.05 for E758C + D1241C, 5109 ± 2060 ms** and 0.9 ± 0.05 for D1241C + D1532C, respectively, $n = 3$–4; compared with 15612 ± 910 ms and 0.90 ± 0.02 for WT, $n = 4$.
*B*, double-cysteine mutations in the outer ring of charge markedly delayed recovery from slow inactivation. The continuous lines are fits of a two-exponential function to the mean data. The time constants and fractional weights (in parentheses) were as follows: E403C + E758C: $\tau_1 = 393.88 \pm 315.65$ ms (0.07 ± 0.06), $\tau_2 = 9898 \pm 3196$ ms** (0.9 ± 0.03); E403C + D1241C: $\tau_1 = 80 \pm 69$ ms (0.33 ± 0.03), $\tau_2 = 1937 \pm 377$ ms* (0.6 ± 0.05); E403C + D1532C: $\tau_1 = 186 \pm 52$ ms (0.3 ± 0.04), $\tau_2 = 2508 \pm 599$ ms* (0.6 ± 0.07); E758C + D1532C: $\tau_1 = 60 \pm 34$ (0.2 ± 0.09), $\tau_2 = 4396 \pm 831$ ms** (0.7 ± 0.05); D1241C + D1532C: $\tau_1 = 59 \pm 19$ ms (0.2 ± 0.03), $\tau_2 = 3969 \pm 354$ ms** (0.8 ± 0.02); $n = 3$–9. In comparison, $\tau_1 = 48 \pm 37$ ms, $A_1 = 0.3 \pm 0.1$, $\tau_2 = 407 \pm 86$ ms and $A_2 = 0.7 \pm 0.1$ for WT ($n = 5$). *C*, time constants of recovery from slow inactivation (corresponding to the slower component of two time constants) in double-cysteine-mutant channels. Recovery from slow inactivation was delayed by 5–25-fold in these double-cysteine-mutant channels. *$P < 0.05$, **$P < 0.01$. *A* represents unit-less fractions.

reasons that slow inactivation may be sensitive to the extracellular $Na^+$. For example, it has been shown that binding of alkali metal cations may inhibit the closing of the slow inactivation gate in wild-type $Na^+$ channels (Townsend & Horn, 1997). Quantitative analysis of the electrostatic field in a sodium channel structural model may provide intuitive insights into structural mechanism. Figure 9 shows a ribbon and stick rendering of the P-segments of domains I and II, with a $-2kTe^{-1}$ electrostatic isopotential contour, represented by the red mesh, between E403 and E758 in the wild-type channel (Fig. 9*A*). This electrostatic potential disappears when E403 and E758 are mutated to cysteines (Fig. 9*B*). The extinction of electrostatic repulsion between outer charged ring residues allows for close proximity, and at least sets a stage for constriction of the outer vestibule, a mechanism for the striking enhancement of slow inactivation observed in the charge neutralization mutants.

## Asymmetrical geometry and electric field

Unlike $K^+$ channels, the $Na^+$ channel is structurally and electrically asymmetrical. Although the electrostatic interactions play an important role in modulation of slow inactivation, the electrical field could be crucially influenced by the asymmetrical geometry of the outer pore. The distance between domain I and domain III is the largest compared with others (Benitah *et al.* 1997). D1241C in domain III appears isolated from the other three residues in the EEDD ring (Fig. 1*B*), consistent with a study by Khan *et al.* (2002). Therefore, the slowest rate of entry into slow inactivation of D1241C compared with the other single-cysteine mutants (Fig. 2*C*), the absence of additional effects on slow inactivation by either charge reversal (Fig. 5*F*) or the double-cysteine substitution E403C + D1241C, can be rationalized by the location of D1241 in the outer pore. We further employed computational simulations to examine the feasibility of an electrostatic contribution by the outer charged ring to slow inactivation gating in a contemporary model

of the $Na^+$ channel pore (online Supplementary Figs 2 and 3). The effect of the D1241R mutation on the local electrostatic potential is the least among the four EEDD residues, consistent with the insignificant difference in recovery from slow inactivation in D1241R mutant channels compared with D1241C (Fig. 5*F*). In contrast, the impact of the change from D1532C to D1532R on the local electrostatic potential is the most profound, consistent with the potent enhancement of slow inactivation by D1532R (Figs 5*E* and 7*B*). On the other hand, the C to R substitutions at E403 and E758 appear to confer an additional effect on electrostatic potentials in the absence of a significant difference in slow inactivation recovery kinetics between E403R and E403C (Fig. 5*F*). However,

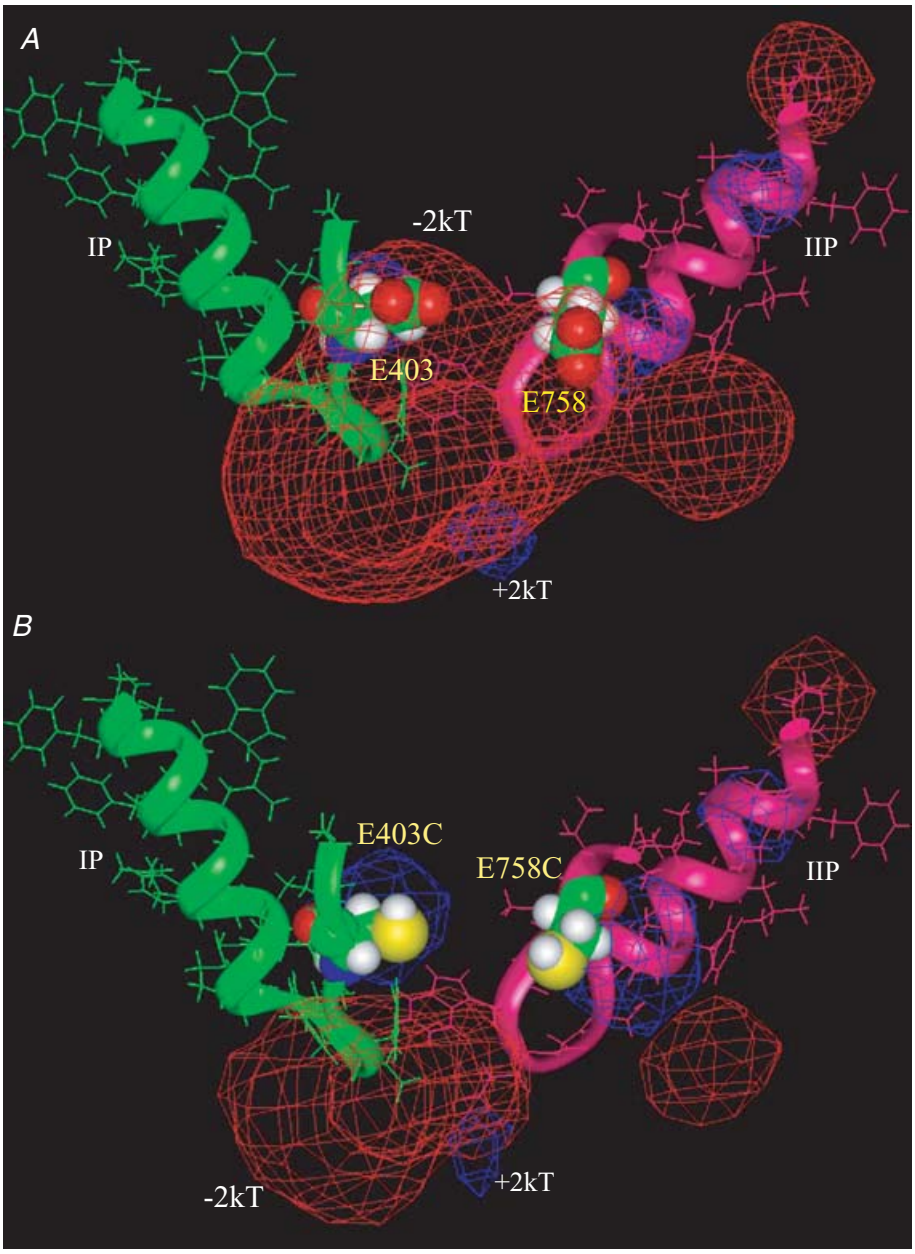


**Figure 9. Significant electrostatic repulsion between E403 and E758**
*A*, the red mesh represents a $-2kT$ isopotential electrostatic surface contour between E403 and E758 in close proximity in the wild-type channel. The P-segments in domains I (green) and II (pink) are shown in a ribbon and stick format. *B*, cysteine mutations at E403 and E758 positions (space-filling format) eliminates $-2kT$ electrostatic potential contour between these two residues, but $-2kT$ electrostatic isopotential surface could be seen around the inner ring of charge (DEKA). The P-segments of domains III–IV as well as S5 and S6 segments in domains I–IV were all included in electrostatic potential calculations with DelPhi, but omitted from this figure for clarity.

E403 appears to have a unique role in slow inactivation (Xiong *et al.* 2003). Moreover, modification of E403C by positively charged MTSET further delayed recovery from slow inactivation (Fig. 4*C*). Thus, we cannot rule out that the structure at the position E403 might be particularly important for slow inactivation.

Unequal enhancement of slow inactivation by different double-cysteine mutants may also be related to asymmetrical geometries and electrostatic fields. The residues in the P-segment of domain IV are mobile, and the distances between residues in domain IV and other domains may be quite large (particularly between domain I and IV) or close, depending on the equilibrium between different states (Benitah *et al.* 1997). The order of distances between P-loops appears to be: I + III > I + IV (or II + IV) > III + IV > I + II. P-loops in domains I and II are functionally close. Domains I and II are thought to be particularly important for slow inactivation (Kontis & Goldin, 1997; O'Reilly *et al.* 1999; also see Mitrovic *et al.* 2000). It has been suggested that if slow inactivation depends on S4 segment mobility, immobilization of the S4 segment by fast inactivation may inhibit slow inactivation (Featherstone *et al.* 1996; Richmond *et al.* 1998). Furthermore, in $Na^+$ channels, the S4 voltage sensors in domains III and IV, but not I and II, are immobilized by fast inactivation (Cha *et al.* 1999). Thus, S4 segments in domains I and II may make a more significant contribution to slow inactivation, although it remains unclear that how S4 segments couple to slow inactivation in $Na^+$ channels.

### A molecular motif regulating the outer pore conformation during slow inactivation

We have shown that the EEDD ring plays a crucial role in modulation of slow inactivation. The natural question is whether this EEDD ring is the slow-inactivation gate or part of the gate. It does not appear to us that the EEDD ring alone constitutes the slow-inactivation gate, although we cannot exclude that it could be part of a slow-inactivation gate if slow inactivation involves a more global rearrangement of the outer pore (Cha & Bezanilla, 1997; Loots & Isacoff, 1998). Instead, it is a molecular motif regulating the open *versus* closed state of the outer pore during slow inactivation of $Na^+$ channels. In *Shaker* $K^+$ channels, the gating motion of S4 is linked to slow inactivation (Pathak *et al.* 2005). The interaction coupling S4 motion and pore closure is likely to be an allosteric effect, possibly involving a strain on the S4–S5 linker and P–S6 loop that subsequently rotate and cause the outer pore to close. In $Na^+$ channels, the S4s of all domains are involved in the slow inactivation, particularly domain I and II (Kontis & Goldin, 1997). Interestingly, the $\mu$-conotoxin with its the strongest interaction sites at E403 and E758 (Dudley *et al.* 1995; Chang *et al.* 1998) can inhibit slow inactivation by serving as a 'splint' to stabilize the open conformation of the outer vestibule (Todt *et al.* 1999).

In summary, E403, E758, D1241 and D1532 in each of the four domains work in concert to regulate the open/closed conformation of the $Na^+$ channel outer pore. In contrast to previous reports of disparate residues in cytoplasmic S4–S5 linkers (Bendahhou *et al.* 2002), S5 (Bendahhou *et al.* 1999) and S6 segments (Hayward *et al.* 1997; Wang & Wang, 1997), the EEDD ring serves as a molecular motif critically modulating slow inactivation in mammalian voltage-gated $Na^+$ channels.

## References


Adelman WJ Jr & Palti Y (1969). The effects of external potassium and long duration voltage conditioning on the amplitude of sodium currents in the giant axon of the squid, *Loligo pealei*. *J Gen Physiol* **54**, 589–606.

Alekov AK, Rahman MM, Mitrovic N, Lehmann-Horn F & Lerche H (2001). Enhanced inactivation and acceleration of activation of the sodium channel associated with epilepsy in man. *Eur J Neurosci* **13**, 2171–2176.

Balser JR, Nuss HB, Chiamvimonvat N, Perez-Garcia MT, Marban E & Tomaselli GF (1996). External pore residue mediates slow inactivation in mu 1 rat skeletal muscle sodium channels. *J Physiol* **494**, 431–442.

Bendahhou S, Cummins TR, Kula RW, Fu YH & Ptacek LJ (2002). Impairment of slow inactivation as a common mechanism for periodic paralysis in DIIS4–S5. *Neurology* **58**, 1266–1272.

Bendahhou S, Cummins TR, Tawil R, Waxman SG & Ptacek LJ (1999). Activation and inactivation of the voltage-gated sodium channel: role of segment S5 revealed by a novel hyperkalaemic periodic paralysis mutation. *J Neurosci* **19**, 4762–4771.

Benitah JP, Ranjan R, Yamagishi T, Janecki M, Tomaselli GF & Marban E (1997). Molecular motions within the pore of voltage-dependent sodium channels. *Biophys J* **73**, 603–613.

Boland LM, Jurman ME & Yellen G (1994). Cysteines in the Shaker $K^+$ channel are not essential for channel activity or zinc modulation. *Biophys J* **66**, 694–699.

Cha A & Bezanilla F (1997). Characterizing voltage-dependent conformational changes in the Shaker $K^+$ channel with fluorescence. *Neuron* **19**, 1127–1140.

Cha A, Ruben PC, George AL Jr, Fujimoto E & Bezanilla F (1999). Voltage sensors in domains III and IV, but not I and II, are immobilized by $Na^+$ channel fast inactivation. *Neuron* **22**, 73–87.

Chang NS, French RJ, Lipkind GM, Fozzard HA & Dudley S Jr (1998). Predominant interactions between mu-conotoxin Arg-13 and the skeletal muscle $Na^+$ channel localized by mutant cycle analysis. *Biochemistry* **37**, 4407–4419.

Choi KL, Aldrich RW & Yellen G (1991). Tetraethylammonium blockade distinguishes two inactivation mechanisms in voltage-activated $K^+$ channels. *Proc Natl Acad Sci U S A* **88**, 5092–5095.

Cordero-Morales JF, Cuello LG, Zhao Y, Jogini V, Cortes DM, Roux B & Perozo E (2006). Molecular determinants of gating at the potassium-channel selectivity filter. *Nat Struct Mol Biol* **13**, 311–318.

Cummins TR & Sigworth FJ (1996). Impaired slow inactivation in mutant sodium channels. *Biophys J* **71**, 227–236.

De Biasi M, Hartmann HA, Drewe JA, Taglialatela M, Brown AM & Kirsch GE (1993). Inactivation determined by a single site in $K^+$ pores. *Pflugers Arch* **422**, 354–363.

Do MT & Bean BP (2003). Subthreshold sodium currents and pacemaking of subthalamic neurons: modulation by slow inactivation. *Neuron* **39**, 109–120.

Dudley SC Jr, Todt H, Lipkind G & Fozzard HA (1995). A mu-conotoxin-insensitive $Na^+$ channel mutant: possible localization of a binding site at the outer vestibule. *Biophys J* **69**, 1657–1665.

Elinder F, Mannikko R & Larsson HP (2001). S4 charges move close to residues in the pore domain during activation in a K channel. *J Gen Physiol* **118**, 1–10.

Featherstone DE, Richmond JE & Ruben PC (1996). Interaction between fast and slow inactivation in Skm1 sodium channels. *Biophys J* **71**, 3098–3109.

Fukuda K, Nakajima T, Viswanathan PC & Balser JR (2005). Compoung-specific $Na^+$ channel pore conformational changes induced by local anesthetics. *J Physiol*.

Gilson MK & Honig BH (1987). Calculation of electrostatic potentials in an enzyme active site. *Nature* **330**, 84–86.

Green WN, Weiss LB & Andersen OS (1987). Batrachotoxin-modified sodium channels in planar lipid bilayers. Ion permeation and block. *J Gen Physiol* **89**, 841–872.

Groenewegen WA, Bezzina CR, Van Tintelen JP, Hoorntje TM, Mannens MM, Wilde AA, Jongsma HJ & Rook MB (2003). A novel LQT3 mutation implicates the human cardiac sodium channel domain IVS6 in inactivation kinetics. *Cardiovasc Res* **57**, 1072–1078.

Harris RE, Larsson HP & Isacoff EY (1998). A permanent ion binding site located between two gates of the Shaker $K^+$ channel. *Biophys J* **74**, 1808–1820.

Hayward LJ, Brown RH Jr & Cannon SC (1997). Slow inactivation differs among mutant Na channels associated with myotonia and periodic paralysis. *Biophys J* **72**, 1204–1219.

Hilber K, Sandtner W, Kudlacek O, Glaaser IW, Weisz E, Kyle JW, French RJ, Fozzard HA, Dudley SC & Todt H (2001). The selectivity filter of the voltage-gated sodium channel is involved in channel activation. *J Biol Chem* **276**, 27831–27839.

Hilber K, Sandtner W, Kudlacek O, Schreiner B, Glaaser I, Schutz W, Fozzard HA, Dudley SC & Todt H (2002). Interaction between fast and ultra-slow inactivation in the voltage-gated sodium channel. Does the inactivation gate stabilize the channel structure? *J Biol Chem* **277**, 37105–37115.

Hirschberg B, Rovner A, Lieberman M & Patlak J (1995). Transfer of twelve charges is needed to open skeletal muscle Na+ channels. *J Gen Physiol* **106**, 1053–1068.

Hoshi T, Zagotta WN & Aldrich RW (1990). Biophysical and molecular mechanisms of Shaker potassium channel inactivation. *Science* **250**, 533–538.

Hoshi T, Zagotta WN & Aldrich RW (1991). Two types of inactivation in Shaker $K^+$ channels: effects of alterations in the carboxy-terminal region. *Neuron* **7**, 547–556.

Hui K, McIntyre D & French RJ (2003). Conotoxins as sensors of local pH and electrostatic potential in the outer vestibule of the sodium channel. *J Gen Physiol* **122**, 63–79.

Isom LL, De Jongh KS, Patton DE, Reber BF, Offord J, Charbonneau H, Walsh K, Goldin AL & Catterall WA (1992). Primary structure and functional expression of the beta 1 subunit of the rat brain sodium channel. *Science* **256**, 839–842.

Kambouris NG, Hastings LA, Stepanovic S, Marban E, Tomaselli GF & Balser JR (1998). Mechanistic link between lidocaine block and inactivation probed by outer pore mutations in the rat micro1 skeletal muscle sodium channel. *J Physiol* **512**, 693–705.

Kass RS (2004). Sodium channel inactivation goes with the flow. *J Gen Physiol* **124**, 7–8.

Khan A, Romantseva L, Lam A, Lipkind G & Fozzard HA (2002). Role of outer ring carboxylates of the rat skeletal muscle sodium channel pore in proton block. *J Physiol* **543**, 71–84.

Kiss L & Korn SJ (1998). Modulation of C-type inactivation by $K^+$ at the potassium channel selectivity filter. *Biophys J* **74**, 1840–1849.

Kontis KJ & Goldin AL (1997). Sodium channel inactivation is altered by substitution of voltage sensor positive charges. *J Gen Physiol* **110**, 403–413.

Lipkind GM & Fozzard HA (2000). KcsA crystal structure as framework for a molecular model of the $Na^+$ channel pore. *Biochemistry* **39**, 8161–8170.

Liu Y, Jurman ME & Yellen G (1996). Dynamic rearrangement of the outer mouth of a $K^+$ channel during gating. *Neuron* **16**, 859–867.

Loots E & Isacoff EY (1998). Protein rearrangements underlying slow inactivation of the Shaker $K^+$ channel. *J Gen Physiol* **112**, 377–389.

Loots E & Isacoff EY (2000). Molecular coupling of S4 to a $K^+$ channel's slow inactivation gate. *J Gen Physiol* **116**, 623–636.

Mitrovic N, George AL Jr & Horn R (2000). Role of domain 4 in sodium channel slow inactivation. *J Gen Physiol* **115**, 707–718.

O'Reilly JP, Wang SY, Kallen RG & Wang GK (1999). Comparison of slow inactivation in human heart and rat skeletal muscle $Na^+$ channel chimaeras. *J Physiol* **515**, 61–73.

O'Reilly JP, Wang SY & Wang GK (2001). Residue-specific effects on slow inactivation at V787 in D2–S6 of Na(v), 1.4 sodium channels. *Biophys J* **81**, 2100–2111.

Olcese R, Latorre R, Toro L, Bezanilla F & Stefani E (1997). Correlation between charge movement and ionic current during slow inactivation in Shaker $K^+$ channels. *J Gen Physiol* **110**, 579–589.

Ong BH, Tomaselli GF & Balser JR (2000). A structural rearrangement in the sodium channel pore linked to slow inactivation and use dependence. *J Gen Physiol* **116**, 653–662.

Pathak M, Kurtz L, Tombola F & Isacoff E (2005). The cooperative voltage sensor motion that gates a potassium channel. *J Gen Physiol* **125**, 57–69.

Patton DE, West JW, Catterall WA & Goldin AL (1992). Amino acid residues required for fast $Na^+$-channel inactivation: charge neutralizations and deletions in the III–IV linker. *Proc Natl Acad Sci U S A* **89**, 10905–10909.

Pavlov E, Bladen C, Winkfein R, Diao C, Dhaliwal P & French R (2005). The pore, not cytoplasmic domains, underlies inactivation in a prokaryotic sodium channel. *Biophys J* **89**, 232–242.

Richmond JE, Featherstone DE, Hartmann HA & Ruben PC (1998). Slow inactivation in human cardiac sodium channels. *Biophys J* **74**, 2945–2952.

Ruff RL, Simoncini L & Stuhmer W (1987). Comparison between slow sodium channel inactivation in rat slow- and fast-twitch muscle. *J Physiol* **383**, 339–348.

Sharp KA & Honig B (1990). Calculating total electrostatic energies with the nonlinear Poisson–Boltzmann equation. *J Phys Chem* **94**, 7684–7692.

Simoncini L & Stuhmer W (1987). Slow sodium channel inactivation in rat fast-twitch muscle. *J Physiol* **383**, 327–337.

Spampanato J, Aradi I, Soltesz I & Goldin AL (2004). Increased neuronal firing in computer simulations of sodium channel mutations that cause generalized epilepsy with febrile seizures plus. *J Neurophysiol* **91**, 2040–2050.

Struyk AF & Cannon SC (2002). Slow inactivation does not block the aqueous accessibility to the outer pore of voltage-gated Na channels. *J Gen Physiol* **120**, 509–516.

Stuhmer W, Conti F, Suzuki H, Wang XD, Noda M, Yahagi N, Kubo H & Numa S (1989). Structural parts involved in activation and inactivation of the sodium channel. *Nature* **339**, 597–603.

Todt H, Dudley SC Jr, Kyle JW, French RJ & Fozzard HA (1999). Ultra-slow inactivation in mu1 $Na^+$ channels is produced by a structural rearrangement of the outer vestibule. *Biophys J* **76**, 1335–1345.

Tomaselli GF, Chiamvimonvat N, Nuss HB, Balser JR, Perez-Garcia MT, Xu RH, Orias DW, Backx PH & Marban E (1995). A mutation in the pore of the sodium channel alters gating. *Biophys J* **68**, 1814–1827.

Townsend C & Horn R (1997). Effect of alkali metal cations on slow inactivation of cardiac $Na^+$ channels. *J Gen Physiol* **110**, 23–33.

Trimmer JS, Cooperman SS, Tomiko SA, Zhou JY, Crean SM, Boyle MB, Kallen RG, Sheng ZH, Barchi RL, Sigworth FJ *et al*. (1989). Primary structure and functional expression of a mammalian skeletal muscle sodium channel. *Neuron* **3**, 33–49.

Tsang SY, Tsushima RG, Tomaselli GF, Li RA & Backx PH (2005). A multifunctional aromatic residue in the external pore vestibule of $Na^+$ channels contributes to the local anesthetic receptor. *Mol Pharmacol* **67**, 424–434.

Vassilev P, Scheuer T & Catterall WA (1989). Inhibition of inactivation of single sodium channels by a site-directed antibody. *Proc Natl Acad Sci U S A* **86**, 8147–8151.

Veldkamp MW, Viswanathan PC, Bezzina C, Baartscheer A, Wilde AA & Balser JR (2000). Two distinct congenital arrhythmias evoked by a multidysfunctional $Na^+$ channel. *Circ Res* **86**, E91–E97.

Vilin YY, Fujimoto E & Ruben PC (2001). A single residue differentiates between human cardiac and skeletal muscle $Na^+$ channel slow inactivation. *Biophys J* **80**, 2221–2230.

Vilin YY, Makita N, George AL Jr & Ruben PC (1999). Structural determinants of slow inactivation in human cardiac and skeletal muscle sodium channels. *Biophys J* **77**, 1384–1393.

Wang SY, Russell C & Wang GK (2005). Tryptophan substitution of a putative D4S6 gating hinge alters slow inactivation in cardiac sodium channels. *Biophys J* **88**, 3991–3999.

Wang DW, Viswanathan PC, Balser JR, George AL Jr & Benson DW (2002). Clinical, genetic, and biophysical characterization of SCN5A mutations associated with atrioventricular conduction block. *Circulation* **105**, 341–346.

Wang SY & Wang GK (1997). A mutation in segment I–S6 alters slow inactivation of sodium channels. *Biophys J* **72**, 1633–1640.

West JW, Patton DE, Scheuer T, Wang Y, Goldin AL & Catterall WA (1992). A cluster of hydrophobic amino acid residues required for fast $Na^+$-channel inactivation. *Proc Natl Acad Sci U S A* **89**, 10910–10914.

Xiong W, Li RA, Tian Y & Tomaselli GF (2003). Molecular motions of the outer ring of charge of the sodium channel: do they couple to slow inactivation? *J Gen Physiol* **122**, 323–332.

Xiong W & Tomaselli GF (2005). Accessibility of the outer vestibule of sodium channels is altered during slow inactivation. *Biophys J* **88**, 602a.

Yang N, George AL Jr & Horn R (1996). Molecular basis of charge movement in voltage-gated sodium channels. *Neuron* **16**, 113–122.

Yang N & Horn R (1995). Evidence for voltage-dependent S4 movement in sodium channels. *Neuron* **15**, 213–218.

Yang Y, Yan Y & Sigworth FJ (1997). How does the W434F mutation block current in Shaker potassium channels? *J Gen Physiol* **109**, 779–789.

Yellen G, Sodickson D, Chen TY & Jurman ME (1994). An engineered cysteine in the external mouth of a $K^+$ channel allows inactivation to be modulated by metal binding. *Biophys J* **66**, 1068–1075.

Zhang Z, Xu Y, Dong PH, Sharma D & Chiamvimonvat N (2003). A negatively charged residue in the outer mouth of rat sodium channel determines the gating kinetics of the channel. *Am J Physiol Cell Physiol* **284**, C1247–C1254.

Zhou Y, Morais-Cabral JH, Kaufman A & MacKinnon R (2001). Chemistry of ion coordination and hydration revealed by a $K^+$ channel-Fab complex at 2.0 A resolution. *Nature* **414**, 43–48.

## Acknowledgements

This work was supported by the National Institutes of Health grants R01 HL50411 (to G.F. Tomaselli). R.A. Li was supported by NIH R01 HL-72857. W. Xiong was supported by a postdoctoral research grant 0225589 U from the American Heart Association. We thank Drs H. A. Fozzard and G. Lipkind for kindly providing us with the coordinate file for generation of the $Na^+$ channel structural model.